JOC Article

Density Functional Study on the Mechanism of the Vanadium-Catalyzed Oxidation of Sulfides by Hydrogen Peroxide

David Balcells, Feliu Maseras,* and Agustí Lledós

Unitat de Química Física, Edifici Cn, Universitat Autònoma de Barcelona, 08193 Bellaterra, Catalonia, Spain

feliu@klingon.uab.es

Received January 16, 2003

A computational study with the Becke3LYP method is carried out on the mechanism of the reaction of complexes V(O)(L)(OOH) and V(O)(LH)(OO) (L = $O(CH)_3N(CH_2)_2O$) with CH_3S-SCH_3, a system that stands as a model for experimental systems where the metal complex contains larger chelating Schiff bases and the substrate is bis(*tert*-butyl) disulfide. The different possible isomers of both the hydroperoxo V(O)(L)(OOH) and the peroxo V(O)(LH)(OO) forms of the catalyst are explored, and the reactivity of the most stable among them with the dimethyl disulfide substrate is studied through location of the corresponding transition states. A large variety of reactive paths happen to exist, though in all cases the reaction takes place through a direct transfer process, with the simultaneous formation of the S−O bond and breaking of the O−O bond being the rate-limiting step.

Introduction

The synthesis of enantiomerically pure sulfoxides is an important reaction because of the widespread application of these compounds as important chiral auxiliaries in organic synthesis.[1−4] There are two major routes for the synthesis of chiral sulfoxides,[5] namely the nucleophilic substitution on chiral sulfur derivatives[6−9] and the asymmetric oxidation of prochiral sulfides.[10−20] The latter method has the advantage of being directly applicable to a wider range of sulfur derivatives. The asymmetric oxidation can be accomplished by reaction of the sulfide with an enantiomerically pure oxidant,[19,20] but the most appealing possibility is the use of an optically inactive oxidant together with a chiral catalyst. However, the lack of a detailed mechanistic understanding hampers the design of more efficient catalytic conditions.

There are a number of catalytic systems able to perform the asymmetric oxidation of sulfides to sulfoxides, involving a variety of transition-metal complexes, reports having been published involving complexes of titanium,[10−12,16,17,21,22] vanadium,[13−15,18,23−27] chromium,[28] manganese,[29] iron,[30] molybdenum,[31] and rhenium[32] as well as enzymatic systems.[33−35] The reaction catalyzed

(1) Carreño, M. C. *Chem. Rev.* **1995**, *95*, 1717.
(2) Colobert, F.; Tito, A.; Khiar, N.; Denni, D.; Medina, M. A.; Martın-Lomas, M.; Ruano, J.-L.; Solladié, G. *J. Org. Chem.* **1998**, *63*, 8918.
(3) Carreño, M. C.; Ribagorda, M.; Posner, G. H. *Angew. Chem., Int. Ed. Engl.* **2002**, *41*, 2753.
(4) Marino, J. P.; McClure, M. S.; Holub, D. P.; Comasseto, U. V.; Tucci, F. C. *J. Am. Chem. Soc.* **2002**, *124*, 1664.
(5) Khiar, N.; Fernández, I.; Alcudia, N.; Alcudia, F. *Adv. Sulfur Chem.* **2000**, *2*, 57.
(6) Andersen, K. K.; Gaffield, W.; Papanikolaou, N. E.; Foley, J. W.; Perkins, R. I. *J. Am. Chem. Soc.* **1964**, *86*, 5637.
(7) Rebière, F.; Riant, O.; Ricard, L.; Kagan, H. B. *Angew. Chem., Int. Ed. Engl.* **1993**, *32*, 568.
(8) Evans, D. A.; Faul, M. M.; Colombo, L.; Bisaha, J. J.; Clardy, J.; Cherry, D. *J. Am. Chem. Soc.* **1992**, *114*, 5977.
(9) Khiar, N.; Alcudia, F.; Espartero, J.; Rodríguez, L.; Fernández, I. *J. Am. Chem. Soc.* **2000**, *122*, 7598.
(10) Kagan, H. B. *Catalytic Asymmetric Synthesis*; Ojima, I., Ed.; Wiley: New York, 1993; p. 203.
(11) Pitchen, P.; Deshmukh, M. N.; Duach, E.; Kagan, H. B. *J. Am. Chem. Soc.* **1984**, *106*, 8188.
(12) Di Furia, F.; Modena, G.; Seraglia, R. *Synthesis* **1984**, 325.
(13) Nakajima, K.; Kojima, K.; Fujita, J. *Chem. Lett.* **1986**, 1483.
(14) Bolm, C.; Binewald, F. *Angew. Chem., Int. Ed. Engl.* **1995**, *34*, 2640.
(15) Cogan, A. D.; Liu, G.; Kim, K.; Backes, B. J.; Ellman, J. A. *J. Am. Chem. Soc.* **1998**, *120*, 8011.
(16) Massa, A.; Siniscalchi, F. R.; Bugatti, V.; Lattanzi, A.; Scettri, A. *Tetrahedron: Asymmetry* **2002**, *13*, 1277.
(17) Capozzi, M. A. M.; Cardellicchio, C.; F., N.; Rosito, V. *J. Org. Chem.* **2002**, *67*, 7289.
(18) Smith, T. S.; Pecoraro, V. L. *Inorg. Chem.* **2002**, *41*, 6754.
(19) Schenk, W. A. *Chem. Eur. J.* **1997**, *3*, 713.
(20) Adam, W.; Korb, M. N.; Roschmann, K. J.; Saha-Moller, C. R. *J. Org. Chem.* **1998**, *63*, 3423.
(21) Saito, B.; Katsuki, T. *Tetrahedron Lett.* **2001**, *42*, 3873.
(22) Adam, W.; Malisch, W.; Roschmann, K. J.; Saha-Moller, C. R.; Schenk, W. A. *J. Organomet. Chem.* **2002**, *661*, 3.
(23) Vetter, A. H.; Berkessel, A. *Tetrahedron Lett.* **1998**, *39*, 1741.
(24) Blum, S. A.; Bergman, R. G.; Ellman, J. A. *J. Org. Chem.* **2003**, *68*, 150.
(25) Skarzewski, J.; Ostrycharz, E.; Siedlecka, R. *Tetrahedron: Asymmetry* **1999**, *10*, 3457.
(26) Skarzewski, J.; Wojazczyńska, E.; Turowska-Tyrk, I. *Tetrahedron: Asymmetry* **2002**, *13*, 369.
(27) Bryliakov, K. P.; Karpyshev, S. A.; Fominsky, A. G.; Tolstikov, A. G.; Talsi, E. P. *J. Mol. Catal. A: Chem.* **2001**, *171*, 73.
(28) Sevvel, R.; Rajagopal, S.; Srinivasan, C.; Alhaji, N. I.; Chellamani, A. *J. Org. Chem.* **2000**, *65*, 3334.
(29) Chellamani, A.; Kylanthaipandi, P.; Rajagopal, *J. Org. Chem.* **1999**, *64*, 2232.
(30) Duboc-Toia, C.; Ménage, S.; Ho, R. Y. N.; Que, L.; Lambeaux, C.; Fontecave, M. *Inorg. Chem.* **1999**, *38*, 1261.
(31) Batigalhia, F.; Zildini-Hernandes, M.; Ferreira, A. G.; Malvestiti, I.; Cass, Q. B. *Tetrahedron* **2001**, *57*, 9669.
(32) Wang, Y.; Espenson, J. *J. Org. Chem.* **2000**, *65*, 104.
(33) van Deurzen, M. P. J.; van Rantwijk, F.; Sheldon, R. A. *Tetrahedron* **1997**, *53*, 13183.
(34) Holland, H. L.; Brown, F. M.; Laksmaiah, G.; Larsen, B. G.; Patel, M. *Tetrahedron: Asymmetry* **1997**, *8*, 683.
(35) Okrasa, K.; Falcimaigne, A.; Guibé-Jampel, E.; Therisod, M. *Tetrahedron: Asymmetry* **2002**, *13*, 519.

10.1021/jo034052t CCC: $25.00 © 2003 American Chemical Society
Published on Web 04/26/2003

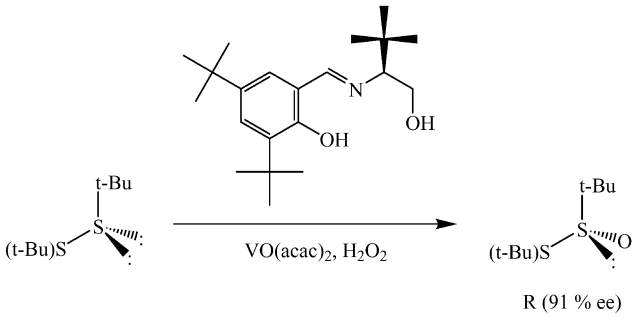

FIGURE 1. Experimental system from Ellman and coworkers.[15]

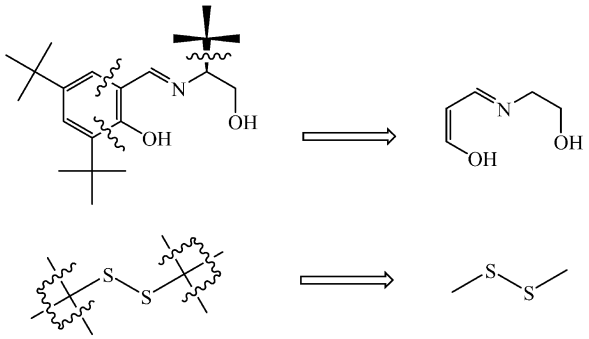

FIGURE 2. Modeling of the real system used in the calculations.

by vanadium species is especially appealing for the computational mechanistic study because of its widespread use and efficiency. Vanadium is, together with titanium, the most common metal center for this type of reactions, and it often operates with the easily available hydrogen peroxide as oxidant. Furthermore, there are some previous experimental studies on vanadium systems that provide useful insight into the reaction mechanism,[24,27] though they fall short of its full characterization.

Most of the catalytic systems involving vanadium respond to the same pattern:[14,15,23−27] there is a precatalyst formed by a 1:1 mix of an oxo complex of vanadium(IV) and a Schiff base, and the oxidant is hydrogen peroxide. The vanadium(IV) oxo complex, usually introduced as $VO(acac)_2$, loses its two labile acac ligands and produces the reactive form of the catalyst, which is a neutral vanadium(V) complex, identified by ^{51}V NMR.[14,15,27] Experimental data indicate that this active species is a 1:1:1 complex containing the oxo vanadium, Schiff base, and peroxide units, and little more is known on its form or on the reaction mechanism.

In this paper, we present a computational study for the particular case of the reaction depicted in Figure 1.[15] The reaction where hydrogen peroxide oxidizes bis(*tert*-butyl) disulfide to *tert*-butyl *tert*-butanethiosulfinate has been shown to be asymmetrically catalyzed by a variety of chiral Schiff bases when mixed with an oxovanadium complex.[15] The system shown in Figure 1 is one example, with good yield and enantiomeric excess.

Computational chemistry has been shown to be a good complement to experiment for the elucidation of reaction mechanisms in homogeneous catalysis.[36−39] Oxidation of sulfides has, however, been little studied so far, and we are aware only of one previous study,[40] which presented calculations on quite unsaturated hydroperoxo compounds of lithium and titanium.

There are nevertheless a number of theoretical studies on the closely related reaction of transition-metal-catalyzed epoxidation by peroxo compounds,[41−52] which is often carried out by similar complexes. Some of the results from these studies on epoxidation have potential implications for the study of sulfide oxidation. Two relevant topics, in particular, have been addressed: the nature of the catalytic species and the type of process by which the oxygen is bound to the substrate. With respect to the active form of the catalyst, the behavior is found to depend on the particular complex: Cr, W catalysts contain an η^2 O−O peroxo unit; Ti catalysts contain an η^1 O−O−H hydroperoxo unit; and the two possibilities seem to exist separated by small energies in other cases. The interaction between catalyst and substrate seems to consist in most cases of a direct transfer of an oxygen atom of the coordinated peroxo (or hydroperoxo) group to the uncoordinated olefin, in contrast with the original proposal of an insertion mechanism with involvement of an intermediate where the substrate is bound to the metal.[53]

It is not clear a priori to what extent these findings for the mechanism of epoxidation hold for the mechanism of oxidation of sulfides. The theoretical calculations presented in this paper will hopefully help to answer this question, as well as provide a mechanistic picture of this process.

Results and Discussion

Modeling of the Real System. The real system,[15] shown in Figure 1, is very large for a full quantum chemical calculation. Because of this, we used the models presented in Figure 2. The potential tridentate character of the Schiff base was preserved, as well as the connection between its three basic centers: the nitrogen and the two

(36) *Computational Modeling of Homogeneous Catalysis*; Maseras, F., Lledós, A., Eds.; Kluwer: Dordrecht, 2002.
(37) Torrent, M.; Solà, M.; Frenking, G. *Chem. Rev.* **2000**, *100*, 439.
(38) Ziegler, T. *J. Chem. Soc., Dalton Trans.* **2002**, 642.
(39) Musaev, D. G.; Morokuma, K. *Top. Catal.* **1999**, *7*, 107.
(40) Jorgensen, K. *J. Chem. Soc., Perkin Trans. 2* **1994**, 117.
(41) Rösch, N.; Di Valentin, C.; Yudanov, I. V. In *Computational Modeling of Homogeneous Catalysis*; Maseras, F., Lledós, A., Eds.; Kluwer: Dordrecht, 2002, p 289.
(42) Gisdakis, P.; Antonczak, S.; Köstlmeier, S.; Herrmann, W. A.; Rösch, N. *Angew. Chem., Int. Ed. Engl.* **1998**, *37*, 2211.
(43) DiValentin, C.; Gisdakis, P.; Yudanov, I. V.; Rösch, N. *J. Org. Chem.* **2000**, *65*, 2996.
(44) DiValentin, C.; Gandolfi, P.; Gisdakis, R.; Rösch, N. *J. Am. Chem. Soc.* **2001**, *123*, 2365.
(45) Gisdakis, P.; Yudanov, I. V.; Rösch, N. *Inorg. Chem.* **2001**, *40*, 3755.
(46) Wu, Y. D.; Lai, D. K. W. *J. Am. Chem. Soc.* **1995**, *52*, 11327.
(47) Wu, Y. D.; Sun, J. *J. Org. Chem.* **1998**, *63*, 1752.
(48) Deubel, D. V.; Sundermeyer, J.; Frenking, G. *J. Am. Chem. Soc.* **2000**, *122*, 10101.
(49) Deubel, D. V.; Sundermeyer, J.; Frenking, G. *Org. Lett.* **2001**, *3*, 329.
(50) Deubel, D. V. *J. Phys. Chem. A* **2001**, *105*, 4765.
(51) Hroch, A.; Gemmecker, G.; Thiel, W. R. *Eur. J. Inorg. Chem.* **2000**, 1107.
(52) Sensato, F. R.; Cass, Q. B.; Longo, E.; Zuckerman-Schpector, J.; Custodio, R.; Andrés, J.; Hernandes, M. Z.; Longo, R. L. *Inorg. Chem.* **2001**, *40*, 6022.
(53) Mimoun, H. *Tetrahedron* **1970**, *26*, 37.

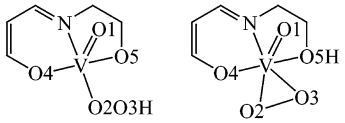

FIGURE 3. Possible hydroperoxo (left) and peroxo (right) forms of the catalyst.

oxygen atoms. The aromatic ring, including its two *tert*-butyl substituents, was eliminated, as well as the additional *tert*-butyl in the aliphatic chain. The eliminated fragments were replaced by hydrogen atoms to avoid dangling bonds. The substrate was also simplified, the *tert*-butyl disulfide being replaced by dimethyl disulfide, CH_3SSCH_3. Preliminary tests of a further simplification of the substrate to HSSH proved it as unreasonable because the acidity of the resulting thiol groups resulted in intramolecular proton-transfer reactions which are impossible in the real system.

We are aware that the modelization used here is likely to reduce substantially, if not completely eliminate, the enantioselectivity of the reaction, which had been shown experimentally to be sensitive to the nature of some of the eliminated substituents. However, we think that this modelization conserves the electronic effects of the reaction. A proper understanding of these electronic effects is a necessary step toward the comprehension of the reaction mechanism. The region absent in our model is likely to have mainly a steric role, and it will be possible to introduce it through QM/MM calculations.[54] These calculations have shown the ability to handle enantioselectivity and regioselectivity in a number of cases,[55−59] but the they require a previous detailed knowledge of the electronic characteristics of the system.

Our computational study is focused on the mechanism by which the oxygen of the hydrogen peroxide is transferred to the sulfide until the sulfoxide molecule is formed. This is the step where the enantioselectivity takes place. Afterward, the catalyst will be regenerated by the entry of a new peroxide unit in a step that is expected to be mechanistically more simple.

Nature of the Catalyst. All available experimental data[14,15,24,27] suggest that the active catalyst consists of a neutral vanadium(V) oxo complex containing as ligands one peroxide unit and one Schiff base. The presence of the peroxide unit in the active catalyst has also been proven to be a requirement in the computational studies on epoxidation.[41] There are, however, still two major possible forms for the catalyst shown in Figure 3. These are V(O)(L)(OOH) (L = $O(CH)_3N(CH_2)_2O$), with a hydroperoxo unit, and V(O)(LH)(OO), with a peroxo unit. As mentioned in the Introduction, there are examples for both of the forms in the case of epoxidation, and therefore, both of them had to be considered as possible candidates for the oxidation of sulfides.

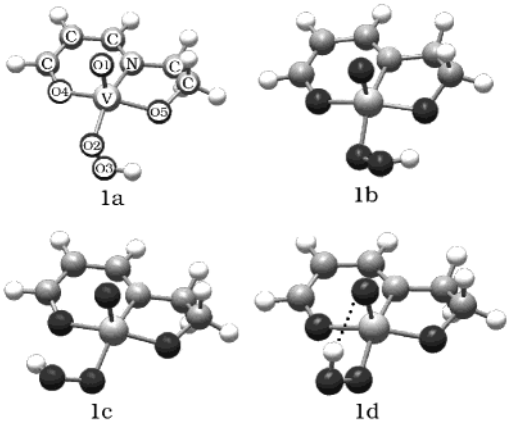

FIGURE 4. Becke3LYP-optimized structure of the four hydroperoxo isomers of the catalyst (**1a**−**d**).

TABLE 1. Selected Optimized Becke3LYP Geometrical Parameters (Å and deg) of the More Stable Isomeric Forms of the Catalyst[a]

	1a	1b	1c	1d	1e	1f
V−O1	1.581	1.584	1.583	1.588	1.600	1.598
V−O2	1.811	1.817	1.804	1.795	1.788	1.831
V−O4	1.912	1.899	1.967	1.933	1.844	2.004
V−O5	1.834	1.830	1.792	1.806	3.558	2.242
V−N	2.123	2.114	2.113	2.124	2.062	2.052
O1−V−O2	108.8	115.0	114.2	105.1	110.0	115.5
O1−V−O4	101.4	105.7	98.2	101.3	120.7	93.5
O1−V−O5	105.3	103.6	107.4	107.6	52.3	83.0
O1−V−N	99.6	98.6	100.6	101.3	96.1	117.3
V−O3	2.431	2.596	2.710	2.814	1.835	1.804
V−O2−O3	95.8	105.0	113.2	121.9	68.7	66.1
O3−O2−V−O5	293.3	59.1	154.1	131.8	−59.9	1.3
energy	0.0	4.1	4.4	4.9	4.4	5.6

[a] The relative free energy in kcal/mol is relative to isomer **1a**.

We first analyzed the hydroperoxo species. The formal oxidation state +5 for the vanadium center, together with the monoanionic character of the hydroperoxo group and the dianionic character of the oxo ligand, require a formal dianionic character of the Schiff base, which is accomplished through the deprotonation of its two alcohol groups, which become therefore alkoxidic. We were able to optimize four distinct isomers of this hydroperoxo form of the catalyst, **1a**, **1b**, **1c**, and **1d**. They are shown in Figure 4, and selected geometrical parameters are included in Table 1. The arrangement around the metal center is practically the same in all cases, the four isomers differing mainly in the conformation around the V−O2 single bond. All complexes have a square pyramidal arrangement around the metal center, with the O1 oxo ligand in the apical position, as shown by the O1−V−X angles close to 90°. All efforts to obtain a different arrangement around vanadium, starting from a geometry with the oxo ligand trans to the Schiff base or to the hydroperoxo ligand, reverted to one of these same isomers. The coordination of the hydroperoxo group in complexes **1a**−**d** is clearly η^1, with the V−O2 distances around 1.8 Å and the V−O3 distances always longer than 2.4 Å.

As mentioned above, the main difference between these four complexes is in the rotation around the V−O2 single bond, indicated by the O3−O2−V−O5 dihedral angle in Table 1. The values are 293.3, 59.1, 154.1, and 131.8°,

(54) Maseras, F. *Chem. Commun.* **2000**, 1821.
(55) Ujaque, G.; Maseras, F.; Lledós, A. *J. Am. Chem. Soc.* **1999**, *121*, 1317.
(56) Carbó, J. J.; Maseras, F.; Bo, C.; van Leeuwen, P. W. N. M. *J. Am. Chem. Soc.* **2001**, *123*, 7630.
(57) Feldgus, S.; Landis, C. R. *J. Am. Chem. Soc.* **2000**, *122*, 12714.
(58) Khoroshun, D. V.; Musaev, D. G.; Vreven, T.; Morokuma, K. *Organometallics* **2001**, *20*, 2007.
(59) Tobisch, S.; Ziegler, T. *J. Am. Chem. Soc.* **2002**, *124*, 13290.

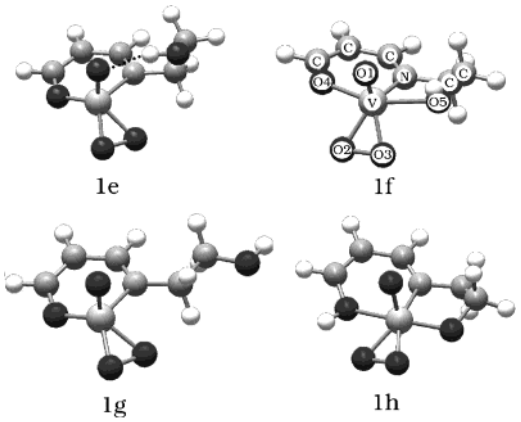

FIGURE 5. Becke3LYP-optimized structure of the four peroxo isomers of the catalyst (**1e**−**h**).

respectively. The existence of two isomers, **1c** and **1d**, with relatively similar values can be explained by the presence in **1d** of a weak hydrogen bond between the peroxide hydrogen and the oxo group at the metal, with an H···O1 distance of 2.372 Å.

There are no X-ray data for V(O)(L)(OOH) species to compare directly with our computed geometries, but the crystal structures of some related complexes have been published. The recently reported[24] structure V(O)(L′)(Cl) (L′ = bulky Schiff base) has a similar square pyramidal arrangement around vanadium and bond distances V−O1, V−O4, V−O5, and V−N of 1.578, 1.827, 1.777, and 2.097 Å, respectively. Our computed geometries thus compare relatively well with available X-ray structures despite the suppression of the bulky substituents in our computational model.

The relative energies of complexes **1a**−**d**, also collected in Table 1, indicate that all of them are within a span of 5 kcal/mol. The interconversion between them is furthermore done through the rotation of a single bond, with low barriers expected. To prove this point, the transition state **2ab** connecting **1a** and **1b** was computed. It has the expected geometry between those of both minima, the value for the O3−O2−V−O5 dihedral angle being 18.6°. The free energy of this transition state is only 7.5 kcal/mol over that of **1a**. Therefore, structures **1a**−**d**, of similar energy, can be interconverted through low barriers, and any of them can represent in principle the most active form of the catalyst.

In fact, we could also optimize a fifth hydroperoxo isomer, **1a′**, where the envelope-shaped five-membered ring including V, N, and O5 had a conformation opposite to that in **1a**. However, the free energy of **1a′** is only 0.2 kcal/mol above that of **1a**, and the barrier connecting both, through transition state **2aa′**, is 2.3 kcal/mol. The structural and energetic similarity, together with the low connecting barrier, prompted us to ignore this **1a′** complex in the rest of this work.

After analyzing the hydroperoxo complexes, we shifted our attention to the peroxo species. To keep the formal oxidation state of vanadium and the neutral character of the complex, the Schiff base has to be monoanionic, and one of its two alcohol groups must retain the proton. We optimized four distinct isomers of this peroxo form of the catalyst, **1e**, **1f**, **1g**, and **1h**. Their structures are presented in Figure 5, and selected geometrical parameters of the two most stable isomers, **1e** and **1f**, are collected in Table 1. In all these species the peroxo group has an η^2 coordination, with both V−O2 and V−O3 distances shorter than 1.9 Å. The arrangement of the peroxo group is very similar in all four isomers. The difference between isomers is associated in this case to the placement of the proton transferred to the Schiff base and its associated ligand. In complexes **1e**−**g**, the proton is attached to the oxygen originally associated to the five-membered ring, which is broken in **1e** and **1g**, while in **1h** it is bound to the oxygen in the six-membered ring. The latter situation is found to be much less stable, with a free energy 30.4 kcal/mol above that of **1a**, probably explainable by the superior acidity expected from a vinylic alcohol. The attachment of the proton to the oxygen in the five-membered ring gives place to three different arrangements, related to the effect of the weakening of the V−O5 bond associated to the protonation of O5. In **1f**, O5 is still bound to vanadium, though with a long distance of 2.242 Å (to be compared with 1.834 Å in **1a**). In **1e** and **1g**, the V−O5 bond is completely broken, the difference between them being that **1e** is stabilized through a hydrogen bond with the oxo ligand O1.

The relative free energies of the peroxo complexes **1e**, **1f**, **1g**, and **1h** with respect to the most stable hydroperoxo complex **1a** are 4.4, 5.6, 9.7, and 30.4 kcal/mol, respectively. Because of their high relative energies, we will omit **1g** and **1h** from further considerations. On the other hand, we consider complexes **1e** and **1f** sufficiently close in energy to **1a** to be feasible candidates for the active form of the catalyst. A last question concerning the relationship between the different candidate complexes is the interconversion between peroxo and hydroperoxo forms. This was investigated through the calculation of **2af**, the transition state connecting **1a** to **1f**. Its transition vector shows the expected formation of the V−O3 bond coupled with the proton transfer from O3 to O5. This transition state has a free energy of 14.8 kcal/mol above **1a**. Though this value is not negligible, we consider it to be still low enough to allow a reasonably fast process. Therefore, complexes **1a**−**f** can in principle coexist in solution, and the choice among them of the active catalyst will depend on their reactivity with the substrate. The six of them must be considered as feasible candidates.

For the sake of simplicity, we will explore in detail in the next subsections the reactivity of the most stable isomer **1a** with dimethyl disulfide and will then use these results as a guide to the study of the reactivity of complexes **1b**, **1c**, **1d**, **1e**, and **1f**, which will be analyzed in a latter subsection.

Insertion or Direct Transfer? As mentioned in the Introduction, the study of the related reaction of transition-metal-catalyzed olefin epoxidation by peroxo compounds[41] has shown that two major mechanistic possibilities exist (Figure 6): the insertion, where the sulfide is "inserted" in the V−OO bond, with the existence therefore of a V−S bond in some moment, and the direct transfer, where an oxygen atom of the OO group is "transferred" to the sulfide without coordination of the latter to the metal center. Both possible reaction mechanisms were investigated for the interaction of the catalyst with dimethyl disulfide.

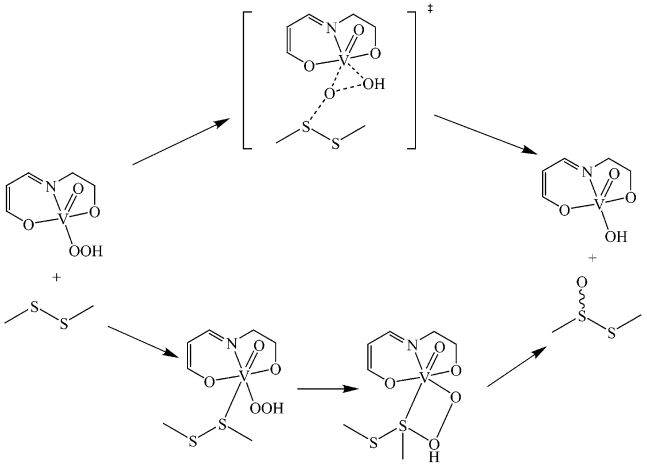

FIGURE 6. Direct transfer (top) and insertion (bottom) reaction mechanisms.

The mechanism of insertion was analyzed first. The most simple formulation of the process starts from an intermediate containing a V−S bond, so we started by searching such species. The formal process of creation of this intermediate is quite simple, consisting of the coordination of sulfide to one of the 5-coordinate isomers of the catalyst **1** reported in the previous subsection, which could in this way become an octahedral 6-coordinate complex. The existence of such a complex would be furthermore no surprise in view of the abundance of complexes containing a V−S chemical bond.[60] We searched for this hypothetical intermediate starting from the geometries of catalyst isomers **1a** and **1e**. The search was not successful. All geometry optimizations, even those starting with analytical calculation of the Hessian, produced a lengthening of the V−S distance, in fact breaking this chemical bond and reverting to the separate reactants stabilized through some long-range interaction. This result is in disagreement with a previous theoretical theoretical study[40] on oxidation of sulfides, where this type of intermediate was located. We think, however, that this discrepancy can be explained by the difference in the model catalyst, which in the previous study was $[TiH_3(O_2H)]$. One could also imagine an insertion mechanism with no previous coordination of sulfide, where the sulfur atom is bound to the metal simultaneously to the formation of the S−O bond. These structures were also investigated, and in this case the geometry optimizations conducted to products.

We were therefore unable to characterize an insertion mechanism for this reaction. We cannot strictly prove that this mechanism does not exist, but we feel that our essays were sufficiently systematic. Furthermore, application of the same tools to the alternative direct-transfer mechanism was successful, as will be shown below. Therefore, we suggest that the reaction does not occur through an insertion mechanism. The lack of efficiency of an insertion mechanism is in agreement with the general observation for systems involved in epoxidation.[41]

The study of the direct-transfer mechanism, also shown in Figure 6, was more successful. In this case, the use as

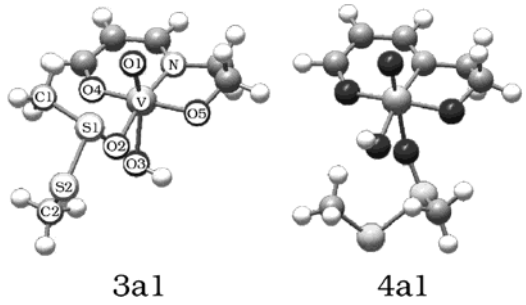

FIGURE 7. Becke3LYP-optimized structure for the transition state of the direct transfer **3a1** and the product **4a1**.

starting geometry of a structure derived from a combination of modified structures of **1a** and dimethyl disulfide allowed the optimization of transition state **3a1**, which is shown in Figure 7. In this transition state, the sulfide attacks oxygen atom O2. This is the oxygen initially attached to the metal. No transition state could be located with sulfide attacking the other oxygen atom O3. Comparison of the geometries of **1a** and **3a1** indicates that this transition state corresponds to oxidation of sulfide. The S1−O2 distance is 2.149 Å in **3a1**, indicating the incipient formation of a chemical bond. The O2−O3 distance goes from 1.449 Å in **1a** to 1.829 Å in **3a1**, consistent with the breaking of the O−O bond. Finally, the V−O3 distance shortens from 2.431 to 2.097 Å, confirming the slippage of the hydroperoxo group leading to the formation of the V−O3 bond. All these structural observations are confirmed in structure **4a1**, also shown in Figure 7, which is the result of the relaxation of transition state **3a1** toward the product side. **4a1**, 22.9 kcal/mol below the reactants, contains in fact the product of the reaction, and it could be formulated as V(O)(L)(OH)($CH_3SS(O)CH_3$). The S1−O2 distance is 1.529 Å, very close to the value in the isolated product $CH_3SS(O)CH_3$, where it is 1.517 Å. This sulfoxide product is weakly bound to vanadium through its oxygen atom, with a long V−O2 distance of 2.597 Å. The O2−O3 and V−O3 distances are 2.950 and 1.807 Å, respectively, showing the complete breaking of the O−O bond and the coordination of a hydroxyl group to vanadium in this product.

Dissociation of the sulfoxide product from **4a1** to produce two separate fragments actually leads to a decrease in the free energy of 4.5 kcal/mol, meaning thus that the dissociated fragments are more stable than the complex. The existence of **4a1** as local minima can seem surprising in view of this result, but it is easily explained by taking into account that the geometry of **4a1** is optimized in the potential energy (not free energy) surface, where it is 7.9 kcal/mol below the separated products. In any case, it is clear that the sulfoxide will be easily replaced in experimental conditions by a solvent molecule, or it will be transferred to another phase. Moreover, replacement of the hydroxyl group by a hydroperoxo group, expected to take place easily in solution, would regenerate the catalyst. Therefore, **4a1** can be considered as the reaction product in this model system.

The most relevant characteristic of transition state **3a1** is its free energy. It is 26.7 kcal/mol above the reactants **1a** + dimethyl disulfide. This value is likely overestimated with respect to experimental conditions in solution because the unfavorable entropic effects of a bimolecular

(60) Simonnet-Jégat, C.; Sécheresse, F. *Chem. Rev.* **2001**, *101*, 2601.

reaction in gas phase are being introduced. In fact, this value goes down to 15.2 kcal/mol when solvation effects are introduced with a PCM method, as will be seen below. In any case, the value is reasonable for a catalyzed reaction. To further confirm the catalytic effect of the vanadium complex, we computed the reaction barrier for the uncatalyzed reaction between hydrogen peroxide and dimethyl disulfide. The uncatalyzed barrier is 40.4 kcal/mol. Therefore, the catalyst is able to lower the barrier by ca. 15 kcal/mol.

Apart from the free energy, other features of transition state **3a1** are also worth of analysis. The quantum mechanical calculations provide certainly insight into the nature of the oxidant attack, electrophilic or nucleophilic, which has been a topic frequently discussed in oxygen-transfer catalysis.[61] In this case, the analysis of the atomic charges indicates that the reaction takes place through electrophilic attack of the hydroperoxo group on the sulfur center. The sulfur atom **S1** has an NPA charge of +0.10 atomic units on the dimethyl disulfide reactant, a value which goes up to +0.48 atomic units on transition state **3a1**. The trend in the NPA charges, which can be arguable for systems where transition metal atoms are present,[62] is fully reproduced by the Mulliken charges, with values of −0.05 au in the reactant and +0.20 au in the transition state. The attacking hydroperoxo group absorbs therefore in the transition state over 0.20 electrons from the sulfide reactant, a result which is clearly associated to an electrophilic attack. The electrophilic nature of the attack is furthermore consistent with the near linear arrangement of the S−O−O group, with a value of 176.6° for the S1−O2−O3 angle in **3a1**. This geometrical arrangement is associated to the essential role played by the σ^* O−O orbital in the interaction.[63] A similar arrangement has been observed in the reaction of sulfide groups with organic peroxides.[64]

All results presented in this subsection suggest that the oxidation of sulfides by this type of vanadium catalysts takes place through direct transfer. The location of a relatively low energy transition state like **3a1** falls short, however, of fully characterizing the reaction mechanism. Other paths can exist within the same direct-transfer mechanism, each of them with its corresponding transition state. These possibilities are systematically explored in the next subsection.

Flexibility of the Transition State. There are several geometrical features in transition state **3a1** (Figure 7) that are not essential to its nature as such that can be modified to produce other structures able to connect reactants to products. To mention one, the modification of the arrangement of the CH_3 and SCH_3 substituents around S1 is likely to be able to produce related structures. In this subsection, the flexibility associated with the arrangement of dimethyl disulfide with respect to the catalyst, or to the internal arrangement of dimethyl disulfide, will be systematically explored taken as starting point structure **3a1**. Readers less interested in technical aspects may skip this section, though its content is essential to demonstrate that the structure proposed for the transition state is the correct one.

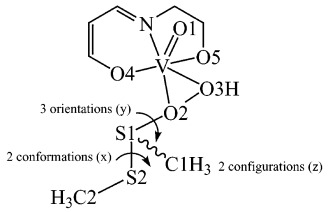

FIGURE 8. Three sources of conformational flexibility in structures **3a**.

The only stereoelectronic requirement for this reaction seems to be that the dimethyl disulfide must approach the catalyst in such a way that the S1−O2−O3 atoms are in a linear arrangement, as indicated above. The value for the S1−O2−O3 angle in **3a1** is 176.6°. All attempts to modify this value, starting geometry optimizations from structures with angles around 120°, reverted rapidly to the linear arrangment. This means that the sulfide must attack O2 in a position anti to O3H. This requirement coincides with that of S_N2 reactions, and in fact, the direct transfer process can be seen as a reaction of this class at O2, with dimethyl disulfide as the entering group and hydroxyl as the leaving group. This linear arrangement was already reported in previous calculations, among them the previous study on oxidation of sulfides[40] and studies on epoxidation of olefins[41] and oxidation of amines[65] by transition-metal complexes containing peroxidic ligands.

Taking into account that the S1−O2−O3 atoms always keep a nearly linear arrangement in the transition state, there are three sources of structural complexity depicted in Figure 8. The first one is associated with the conformation of the substrate concerning the rotation around the S1−S2 single bond and can be numerically characterized by the O2−S1−S2−C2 dihedral angle, which will be labeled as **x**. The second source of complexity is related to the orientation of the entering group with respect to the catalyst, defined by the rotation around the O2−S1 bond, and we have characterized it with the V−O2−S1−S2 dihedral angle, labeled as **y**. The third structural variation is associated to the configuration at the S1 center, and can be measured with the C1−S1−S2−O2 dihedral angle, labeled as **z**. We carried out a preliminary study to obtain the possible values of each of the three parameters **x**, **y**, and **z**. For **x**, a rigid scan on **3a1** with the rest of the geometrical parameters frozen produced two local minima with values of −30° (**x1**) and 170° (**x2**). The rigid scan corresponding to **y** could not be carried out directly on **3a1** because of excessive steric strain, but its performance on one of its modifications yielded three local minima around 180° (**y1**), −90° (**y2**), and 50° (**y3**). For **z**, there was no need for scan, as the possible values must be around 120° (**z1**) and −120° (**z2**) for a tetrahedral center like S1.

These preliminary calculations indicate thus that there are in principle 12 possible conformations of transition state **3a**, corresponding to the product of two values for

(61) Adam, W.; Golsch, D.; Sundermeyer, J.; Wahl, G. *Chem. Ber.* **1996**, *129*, 1177.
(62) Maseras, F.; Morokuma, K. *Chem. Phys. Lett.* **1992**, *195*, 500.
(63) Bach, R. D.; Wolber, G. J.; Coddens, B. A. *J. Am. Chem. Soc.* **1984**, *106*, 6098.
(64) Baboul, A. G.; Schlegel, H. B.; Glukhovtsev, M. N.; Bach, R. D. *J. Comput. Chem.* **1998**, *19*, 1353.
(65) Thiel, W. R.; Krohn, K. *Chem. Eur. J.* **2002**, *8*, 1049.

TABLE 2. Selected Optimized Becke3LYP Geometrical Parameters (Å and deg) and Energies of the 10 Different Transition States Associated to 1a[a]

	O2−S1	O2−O3	O2−S1−S2−C2 (**x**)	V−O2−S1−S2 (**y**)	C1−S1−S2−O2 (**z**)	G_{rel}
x1y1z1	2.149	1.829	−31.2	177.2	101.1	26.7
x1y1z2	2.137	1.835	24.8	174.9	−99.9	27.5
x1y2z2	2.119	1.840	16.9	94.9	−93.2	27.6
x1y2z1	2.112	1.843	−15.9	−87.1	93.6	27.7
x2y1z1	2.110	1.848	170.2	177.2	95.9	28.4
x2y1z2	2.105	1.853	−170.8	−176.6	−98.6	28.6
x2y2z1	2.078	1.860	172.0	−107.1	91.3	28.9
x2y2z2	2.085	1.857	−170.8	95.9	−91.5	29.5
x2y3z2	2.082	1.846	−147.1	−33.6	−103.6	30.1
x2y3z1	2.083	1.851	145.1	38.0	105.5	30.2

[a] Free energy in kcal/mol is relative to **1a** + dimethyl disulfide.

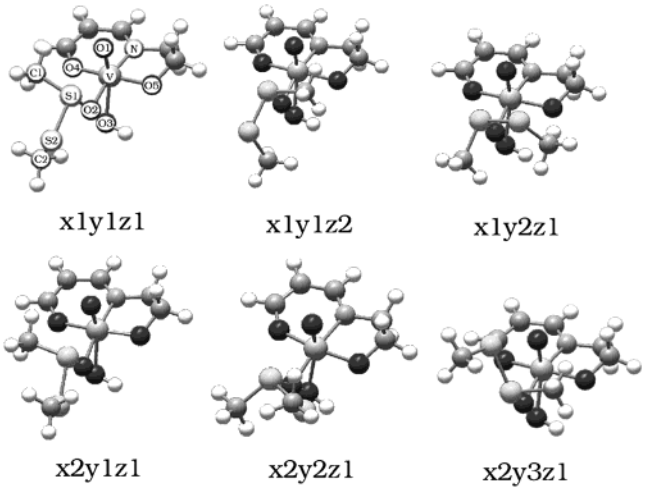

FIGURE 9. Becke3LYP-optimized structures for selected conformational variations of transition state **3a**.

x times three values for **y** times two values for **z**. All of them were searched for in full-geometry optimizations starting from the corresponding geometries. Ten distinct transition states were located, the other two calculations reverting to other geometries. Energies and geometrical parameters are presented in Table 2, and a selection of the structures is shown in Figure 9. The structures, which are in fact variations of transition state **3a**, are labeled according to the starting values of **x**, **y**, and **z** of the corresponding geometry optimizations. **3a1**, presented in the previous subsection, corresponds in this terminology to **x1y1z1**. It can be seen in Table 2 that the parameters corresponding to the main two bonds being formed and broken, O2−S1 and O2−O3, respectively, are very similar for all these structures and close to the values reported above for **x1y1z1**. All values for O2−S1 are within a span of 0.071 Å, and the range for O2−O3 is even smaller, 0.038 Å. All structures correspond therefore to conformational variations of the transition state for the reaction of oxidation of sulfide.

Dihedral angles **x** and **y** are not completely independent, and in fact, the combination of the values **x1** and **y3** creates a strong steric repulsion that makes impossible the convergence of structures **x1y3z1** and **x1y3z2**. The free energies collected in Table 2 clearly indicate that the preferred values for **x** and **y** are **x1** and **y1**, respectively. As a result, the most stable transition states are **x1y1z1** and **x1y1z2**. Concerning the value of **z**, associated with the absolute configuration of the sulfoxide, it must be said that the small difference of 0.8 kcal/mol between **x1y1z1**, leading to the **R** product, and **x1y1z2**, leading to the **S** product, shows the small stereoselective power of the model system, in absence of the *tert*-butyl substituents of the experimental system (Figure 2). In fact, the chirality computed with this model is not relevant because, the model Schiff base L being not chiral, the enantiomeric form of the catalyst would be present in the same amount in solution. A last conclusion to be extracted from Table 2 is that the value for dihedral angle **x**, associated with rotation around the S1−S2 single bond, seems to be the most critical, because the least stable **x1** structure is still lower in energy than the most stable **x2** geometry.

Reactivity of Other Isomers of the Catalyst. The results presented in the previous subsection apply strictly to the variation of transition state **3a**, related to catalyst **1a**. However, we had seen before that **1a**, despite being the most stable isomer, is not necessarily the active form of the catalyst. The reactivity of other catalysts had to be thus explored. For these other forms of the catalyst we did not carry the full study of the flexibility but used the information learned from the systematic study of **3a**.

The transition states associated with isomers **1b**, **1c**, **1d**, **1e**, and **1f** were searched. The starting parameters for the geometry optimization were −30° for O2−S1−S2−C2 (**x1**) and 180° for V−O2−S1−S2 (**y1**), following the findings for **3a** presented in the previous subsection. For the dihedral angle C1−S1−S2−O2 (**z**), ruling the absolute configuration at S1, both possible values were used, and only the most stable transition will be presented in each case. The transition-state optimization was successful for the structures related to the **1b**, **1c**, and **1e** forms of the catalyst, producing the structures **3b1**, **3c1**, **3e1**, and **3e2** (Figure 10 and Table 3). No transition states could be located associated with **1d** and **1f**, the calculations converging to **3c1** and **3e1**, respectively. Both **1d** and **1f** seem quite sterically hindered for interaction with the sulfide, this result being therefore not surprising. For the case of the peroxo complex **1e**, two transition states are presented, **3e1** and **3e2**, each of them associated with the attack on one of the peroxidic oxygen atoms O2, and O3, respectively. Table 3 shows that all these geometries present reasonable values for the bonds being formed and broken. The O2−S distance of the bond being formed is always between 2.109 and 2.248 Å, corresponding to O3−S1 in the case of **3e2** and to O2−S1 in all other cases. The O2−O3 distance, associated with the bond being broken, is always between

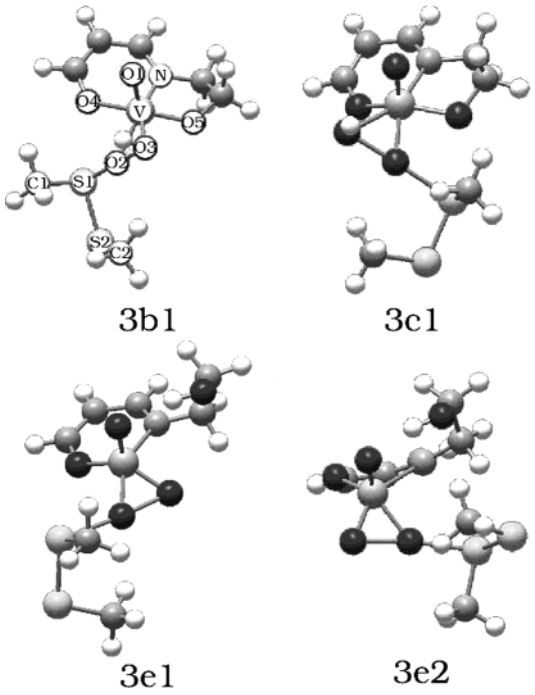

FIGURE 10. Becke3LYP optimized structures for the transition states connected to the less stable isomers of the catalyst.

1.776 and 1.829 Å. All structures correspond therefore to transition states of the oxidation of sulfide.

The optimized values for the dihedral angles **x** and **y** presented in Table 3 are reasonably close to the corresponding starting value, with the notable exception of the V−O2−S1−S2 dihedral angle in **3e2**, which is 91.3°, very far from the initial 180°. This deviation is likely related to strong steric repulsions between the methyl group associated to C1 and the Schiff base. In fact, the dihedral angle V−O2−S1−S2 shows a larger variation than O2−S1−S2−C2, probably suggesting that rotation around O2−S1 is critical in modulating the steric interactions between substrate and catalyst.

Concerning the free energies collected in Table 3, it is worth mentioning that in all cases the computed barrier is well below the 40.5 kcal/mol associated to the uncatalyzed reaction. Therefore, all isomers of the catalyst have catalytic properties. As for the comparison between the computed structures, the most stable transition state is **3a1**, followed by **3e1**, **3e2**, **3c1**, and **3b1**. **3e1** is 2.5 kcal/mol above **3a1**, and **3b1** is 7.3 kcal/mol. These calculations indicate therefore that in this model system the reaction would proceed through transition state **3a1**, connected to the hydroperoxo isomeric form **1a** of the catalyst. Nevertheless, caution must be taken to avoid overinterpretation of these results, in particular taking into account that the bulky substituents of the real system have been cut off in our model system. We feel quite confident in saying that **3a1** is the preferred transition state for electronic reasons. However, the lack of steric interactions in this model system does not allow us to discard an eventual role in experimental systems of transition state **3e1** or, especially, the variations of **3a** described in the previous subsection. A more detailed analysis of **3e1** proves that in this case the attack of the peroxo group on the sulfide is also electrophilic, with the charge on the S1 sulfur going from +0.10 (reactant) to +0.37 au (transition state) with the NPA method and from −0.05 (reactant) to +0.12 au (transition state) with the Mulliken method.

The Reaction Mechanism after the Oxygen Transfer. When **3a1** was first presented, it was mentioned that its relaxation led directly to structure **4a1**, containing the sulfoxide product already formed and weakly coordinated to the metal. In this subsection, we will analyze what happens with transition states **3b1**, **3c1**, **3e1**, and **3e2** when relaxed toward products.

The behavior of structures associated to the peroxo catalyst **1e**, namely **3e1** and **3e2**, was quite similar to that of **3a1** mentioned above. Both transition states relaxed directly to structures that can be considered as the reaction product which we label as **4e1** and **4e2**. The free energies are, respectively, 19.1 and 14.0 kcal/mol below **1a** + CH_3SSCH_3. In both cases, the S−O bond is practically formed with S1−O distances of 1.557 Å in the case of **4e1**, and 1.551 Å in the case of **4e2**, and the sulfoxide is weakly coordinated to vanadium through the oxygen atom in a position trans to the oxo ligand.

The result was different when the same treatment was applied to structures **3b1** and **3c1**. Relaxation of **3b1** produced complex **5b1**, included in Figure 11. The S1−O2, O2−O3, and V−O2 distances of 1.569, 2.845, and 2.032 Å indicate that the product is nearly formed and coordinated to the metal, as in the cases mentioned above. However, the relative free energy of **5b1** is not clearly below the reactants, as would correspond to the overall exothermic process, but it is in fact 1.47 kcal/mol above **1a** + CH_3SSCH_3. This seemingly contradiction can be easily explained by inspecting the geometry presented in Figure 11. **5b1** differs from all the structures presented above in the arrangement of ligands around vanadium. The hydroxyl is not trans to the nitrogen atom of the Schiff base, but to one of the alkoxy groups, and the oxo group is trans to the other alkoxy, with the sulfoxide molecule ending up trans to the nitrogen atom. This is not the energetically optimal arrangement, and this explains the relatively high energy of **5b1**. A further exploration of the potential energy hypersurface showed that **5b1** is connected directly to product **4a1** through transition state **6b1**, which has a relative energy of 9.1 kcal/mol. Therefore, a reaction path can be defined starting from the reactants **1b** + CH_3SSCH_3 and reaching product **4a1** through transition state **3b1**, intermediate **5b1** and transition state **6b1**. It is worth remarking that the energy of the second transition state **6b1**, 9.1 kcal/mol, is more than 20 kcal/mol below that of transition state **3b1**, 34.0 kcal/mol. Therefore, the limiting step of the reaction path, where the rate of the whole process is decided, is still defined by **3b1**.

Relaxation of transition state **3c1** toward products yields results very similar to those of **3b1**. In this case, the intermediate **5c1** (also presented in Figure 11), has a relative energy of −0.2 kcal/mol, and the transition state connecting it to product **4a1** has a relative energy of 7.7 kcal/mol.

The evolution toward products of the different transition states **3** is therefore quite diverse, with a single step in some cases and the presence of an intermediate in other cases. It is nevertheless clear that transition state **3**, corresponding to the breaking of the O−O bond and

TABLE 3. Selected Optimized Becke3LYP Geometrical Parameters (Å and deg) and Energies of Selected Transition States Associated to Different Isomeric Forms of the Catalyst[a]

	O2−S1	O3−S1	O2−O3	O2−S1−S2−C2 (**x**)	V−O2−S1−S2 (**y**)	C1−S1−S2−O2 (**z**)	G_{rel}
3a1	2.149	1.829	3.975	−31.2	177.2	101.1	26.7
3b1	2.109	1.798	3.907	20.0	139.3	−94.8	34.0
3c1	2.143	1.779	3.922	−21.8	−157.5	96.2	33.9
3e1	2.248	1.776	4.020	17.1	139.4	−92.4	29.2
3e2	3.907	1.784	2.133	1.6	91.3	−89.9	33.4

[a] The free energy in kcal/mol is relative to **1a** + dimethyl disulfide.

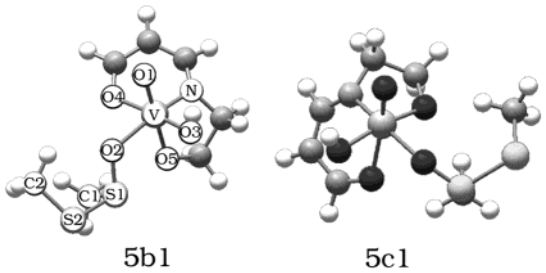

FIGURE 11. Becke3LYP-optimized structures for the intermediates between rate-limiting transition states and products.

the formation of the S−O bond has in all possible cycles the highest energy and corresponds therefore to the rate-limiting step. The best path will be therefore that with the lowest energy for this particular step. The definition of the full path from reactant to products is necessary for the sake of completeness, but the results presented here prove that the eventual presence of an intermediate after the critical transition state will not have any effect on the outcome of the reaction.

Improvements to the Computational Method. The choice of a computational level is always the result of the balance between the desired accuracy of the result and the computational effort necessary to obtain it. In this subsection, we analyze two particular aspects of the computational level chosen, namely the nature of the basis set and the lack of solvation effects.

The basis set used in all the calculations presented above, which we label as basis set I, and that will be fully defined in the Computational Details, was valence double-ζ for all atoms, supplemented with polarization d shells on sulfur, oxygen, and nitrogen. An effective core potential was used to replace the innermost electrons of sulfur and vanadium. This basis set had a total of 223 basis functions. Previous works have shown that large basis sets may be required for reactions involving sulfoxides,[66] and because of this we tested a larger basis set II. Basis set II contains an all electron description for sulfur and introduces diffuse s and p shells in sulfur, oxygen and nitrogen atoms. Basis set II has a total of 265 basis functions.

A total of 15 structures were recalculated with basis set II on the frozen geometries obtained with basis set I. This included the most stable catalyst forms **1a** and **1e**, all conformational variations of transition state **3a1**, transition state **3e1** and products **4a1** and **4e1**. All relative energies are collected in the Supporting Information. The critical potential energy of the transition states with respect to the reactants is reduced by an amount between 0.7 and 1.0 kcal/mol, but in no case does this lead to changes in the ordering of the more stable structures. Structure **3a1** remains clearly as the most stable transition state.

The fact that our calculations are in the gas phase and the experimental reactions take place in solution is also a source of error. We evaluated the effect that a water solvent could have by carrying out single-point PCM calculations[67] on the 15 frozen gas-phase structures mentioned above. All relative free energies are also collected in the Supporting Information. In this case, changes in the absolute barriers are more significant, with the relative free energy of **3a1** with respect to the reactants going down by more than 10 kcal/mol (26.7 kcal/mol in gas phase vs 15.2 kcal/mol in solution). The preference of **3a1** over all other transition states is nevertheless unchanged.

Therefore, these supplementary calculations prove that the main trends in our results are not altered by basis set or solvation effects.

Conclusions

The computational study of the oxidation of dimethyl disulfide by simplified models of the experimental V(O)(L′)(OOH) and V(O)(L′H)(OO) (L′ = bulky Schiff base) systems gives useful information on the experimental reaction mechanism. The calculations are conclusive in favoring the direct transfer mechanism with respect to the alternative insertion mechanism. The sulfur atom is therefore never directly attached to the metal in this catalytic cycle. The theoretical study is also clear in indicating that the breaking of the O−O bond of the oxidant and the formation of the S−O bond of the product take place simultaneously and that this process is the rate-limiting step of the catalytic cycle.

This study has also shown the large conformational complexity of the system. A number of different reaction paths have been characterized, some of them with small differences in the free energy barrier, and the existence of additional reaction paths, with slightly higher barriers is likely. In our model system, the lowest barrier corresponds to the path going directly from the reactants **1a** + dimethyl disulfide to the product **4a1** through transition state **3a1**. However, we consider that steric effects are likely to play an important role in the relative energetics of transition states, and that their presence in the real systems could seriously alter the nature of the most favored path. The current work is nevertheless also useful in this concern, because it identifies the

(66) Cubbage, J. W.; Guo, Y.; McCulla, R. D.; Jenks, W. S. *J. Org. Chem.* **2001**, *66*, 8722.

(67) Miertus, S.; Scrocco, E.; Tomasi, J. *Comput. Phys.* **1981**, *55*, 117.

possible paths and quantifies the energy differences between them when only electronic effects are taken into account.

The theoretical determination of the optimal reaction paths for a given experimental system and the consequent prediction of the enantioselectivity will require the introduction of the complete real system in the calculation. This seems an appropriate challenge for quantum mechanics/molecular mechanics methods, and we are currently working in our laboratory in this project.

Computational Details

All calculations were carried out using the Becke3LYP[68,69] density functional as implemented within the Gaussian98 package.[70] Two basis sets were used. Most calculations were carried out with basis set I. In basis set I, an effective core potential was used to replace the 10 innermost electrons of vanadium[71] and sulfur.[72] The valence double-ζ basis set associated to the pseudopotential in the program,[70] with the contraction labeled as LANL2DZ was used for these two elements, supplemented with a d shell for sulfur.[73] The 6-31G-(d) basis set was used for oxygen and nitrogen[74,75] and 6-31G for carbon and hydrogen.[74] The basis set was thus valence double-ζ for all elements, with additional polarization d shells for all atoms attached to the metal or directly involved in the oxygen transfer process. Basis set II, used only in a set of single-point calculations, was an extension of basis set I where the basis sets for sulfur, nitrogen, and oxygen was replaced by 6-31+G(d). That is, the effective core potential on sulfur was replaced by an all-electron basis,[76] and additional diffuse s, p shells[77] were added to atoms containing polarization functions in basis set I.

All geometry optimizations were full, with no restrictions. Stationary points located in the potential hypersurface were identified as true minima or transition states through vibrational analysis. All energetic values reported correspond to free energies at 25 °C and 1 atm. Absolute and relative potential energy values, as well as relative zero-point energy corrections, and enthalpies are reported in the Supporting Information.

Acknowledgment. Financial support from the Spanish MCyT (Project No. BQU2002-04110-CO2-02) and FEDER and the Catalan DURSI (Project No. 2001SGR00179) is acknowledged. F.M. also acknowledges the support of DURSI.

Supporting Information Available: A table containing all computed relative thermodynamic magnitudes, as well as tables with the Becke3LYP-optimized geometries (Cartesian coordinates) and absolute potential energies for the 32 compounds labeled in the text. This material is available free of charge via the Internet at http://pubs.acs.org.

JO034052T

(68) Becke, A. D. *J. Chem. Phys.* **1993**, *98*, 5648.
(69) Lee, C.; Parr, R. G.; Yang, W. *Phys. Rev.* **1988**, *37*, B785.
(70) Frisch, M. J.; Trucks, G. W.; Schlegel, H. B.; Scuseria, G. E.; Robb, M. A.; Cheeseman, J. R.; Zakrzewski, V. G.; Montgomery, J. A.; Stratmann, R. E., Jr.; Burant, J. C.; Dapprich, S.; Millam, J. M.; Daniels, A. D.; Kudin, K. N.; Strain, M. C.; Farkas, O.; Tomasi, J.; Barone, V.; Cossi, M.; Cammi, R.; Mennucci, B.; Pomelli, C.; Adamo, C.; Clifford, S.; Ochterski, J.; Petersson, G. A.; Ayala, P. Y.; Cui, Q.; Morokuma, K.; Malick, D. K.; Rabuck, A. D.; Raghavachari, K.; Foresman, J. B.; Cioslowski, J.; Ortiz, J. V.; Stefanov, B. B.; Liu, G.; Liashenko, A. Piskorz, P.; Komaromi, I.; Gomperts, R.; Martin, R. L.; Fox, D. J.; Keith, T. Al-Laham, M. A.; Peng, C. Y.; Nanayakkara, A.; Gonzalez, C.; Challacombe, M.; Gill, P M. W.; Johnson, B.; Chen, W.; Wong, M. W.; Andres, J. L.; Gonzalez, C.; Head-Gordon, M.; Replogle, E. S.; Pople, J. A. *Gaussian*; Gaussian, Inc.: Pittsburgh, PA, 1998.
(71) Hay, P. J.; Wadt, W. R. *J. Chem. Phys.* **1985**, *82*, 299.
(72) Wadt, W. R.; Hay, P. J. *J. Chem. Phys.* **1985**, *82*, 284.
(73) Höllwarth, A.; Böhme, M.; Dapprich, S.; Ehlers, A. W.; Gobbi, A.; Jonas, V.; Köhler, K. F.; Stegmann, R.; Veldkamp, A.; Frenking, G. *Chem. Phys. Lett.* **1993**, *208*, 237.
(74) Hehre, W. J.; Ditchfield, R.; Pople, J. A. *J. Phys. Chem.* **1972**, *56*, 2257.
(75) Hariharan, P. C.; Pople, J. A. *Theor. Chim. Acta* **1973**, *28*, 213.
(76) Francl, M. M.; Pietro, W. J.; Hehre, W. J.; Binkley, J. S.; Gordon, M. S.; Defrees, D. J.; Pople, J. A. *J. Phys. Chem.* **1982**, *77*, 3654.
(77) Clark, T.; Chandrasekhar, J.; Spitznagel, G. W.; Schleyer, P. v. R. *J. Comput. Chem.* **1983**, *3*, 294.